ChemComm

View Online
Dynamic Article Links

Cite this: *Chem. Commun.*, 2011, **47**, 8910–8912

www.rsc.org/chemcomm

COMMUNICATION

A strategy to design highly efficient porphyrin sensitizers for dye-sensitized solar cells†

Yu-Cheng Chang,[a] Chin-Li Wang,[b] Tsung-Yu Pan,[a] Shang-Hao Hong,[b] Chi-Ming Lan,[a] Hshin-Hui Kuo,[b] Chen-Fu Lo,[b] Hung-Yu Hsu,[a] Ching-Yao Lin*[b] and Eric Wei-Guang Diau*[a]

Received 11th May 2011, Accepted 6th June 2011
DOI: 10.1039/c1cc12764k

We designed highly efficient porphyrin sensitizers with two phenyl groups at *meso*-positions of the macrocycle bearing two *ortho*-substituted long alkoxyl chains for dye-sensitized solar cells; the *ortho*-substituted devices exhibit significantly enhanced photovoltaic performances with the best porphyrin, LD14, showing J_{SC} = 19.167 mA cm^{-2}, V_{OC} = 0.736 V, FF = 0.711, and overall power conversion efficiency η = 10.17%.

Because of their excellent light-harvesting property with intense absorption throughout the visible to the near-IR region, various porphyrins have been designed and applied for dye-sensitized solar cells (DSSC).[1] Optimization of the device performance for a push–pull zinc porphyrin (YD2) has attained power conversion efficiency η = 11.0%,[2] which is a new milestone for a porphyrin-based DSSC to compete with the highly efficient ruthenium-based DSSC developed almost two decades ago. This great performance of YD2 is due to its superior light-harvesting ability through introduction of a diarylamino group at the *meso*-position of the porphyrin ring.[3] A similar approach was applied in introducing a pyrene moiety through a π-conjugated link coupled to a porphyrin core (LD4) to enhance greatly the light-harvesting ability beyond 800 nm.[4] The open-circuit voltages (V_{OC}) of those highly efficient porphyrin dyes were reported,[3,4] however, to be significantly less than that of the commonly used ruthenium dye N719. Mozer *et al.*[5] stated that the significantly diminished electron lifetime is the main reason accounting for the smaller V_{OC} of porphyrins; they proposed that I_3^- in the electrolyte might be attached to the positively charged Zn-center of the porphyrin core for an efficient electron interception from the TiO_2 surface to occur. Tian and co-workers,[6] who reviewed the photovoltaic results for many organic and ruthenium sensitizers, concluded that V_{OC} can be improved upon decreasing the charge recombination and increasing the efficiency of electron injection with an appropriate design for an organic dye. To tackle this problem, we introduce in this communication a new concept to design a zinc porphyrin sensitizer with long alkoxyl chains to protect the porphyrin core for a retarded charge recombination and also to decrease effectively the dye aggregation for an efficient electron injection.

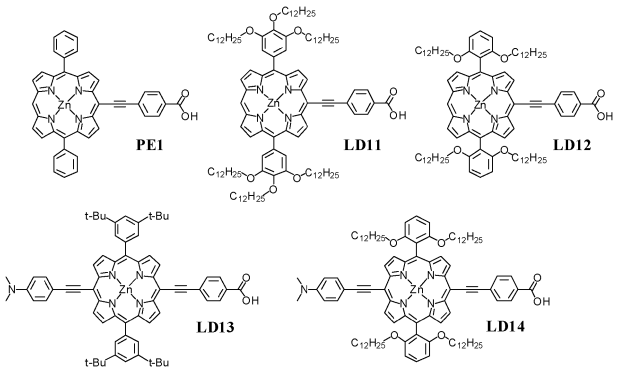

Chart 1 Molecular structures of PE1 and the LD11–LD14 porphyrins.

Chart 1 shows the molecular structures of the proposed porphyrins based on this design. The core structures are based on PE1 reported elsewhere,[7] with two phenyl substituents bearing two dodecoxyl (–$OC_{12}H_{25}$) chains at the *ortho*-position of each phenyl group (labeled LD12); the reference porphyrin (LD11) has three dodecoxyl groups at the *meta*- and *para*-positions of each phenyl group. We designed similarly a push–pull porphyrin (LD14) based on the structure of LD13 reported elsewhere.[8] The syntheses of these porphyrins are similar to those reported elsewhere;[7-9] details of the procedures are given in ESI.† Fig. S1† shows UV/vis absorption spectra of the four porphyrins in THF solution; the related spectral data are summarized in Table S1.† We investigated the electrochemical properties of these porphyrins using cyclic voltammetry (CV); the cyclic voltammograms are shown in Fig. S2† with the resulting oxidation and reduction potentials summarized in Table S1.† Based on the CV results, a potential-level diagram showing the HOMO and the LUMO of each porphyrin is presented in Fig. 1. These CV results indicate that the porphyrins with long alkoxyl chains attached at the *ortho*-positions of the phenyl rings have more negative reduction and oxidation potentials than those with long

[a] *Department of Applied Chemistry and Institute of Molecular Science, National Chiao Tung University, Hsinchu 300, Taiwan. E-mail: diau@mail.nctu.edu.tw; Fax: +886 3-572-3764; Tel: +886 3-513-1524*
[b] *Department of Applied Chemistry, National Chi Nan University, Puli, Nantou Hsien 54561, Taiwan. E-mail: cyl@ncnu.edu.tw; Fax: +886 49-2917956; Tel: +886 49-2910960 ext. 4152*
† Electronic supplementary information (ESI) available: Fig. S1–S10, Tables S1–S5, and experimental details. See DOI: 10.1039/c1cc12764k

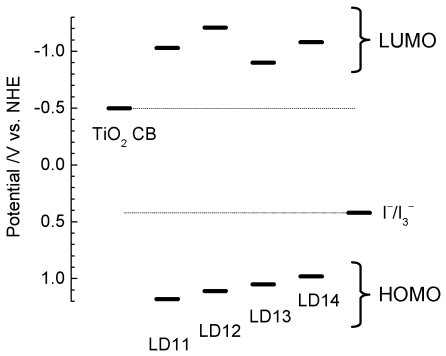

Fig. 1 Potential-level diagram of the LD11–LD14 porphyrins, the TiO_2 conduction band, and the redox mediator.

alkoxyl chains attached at *meta*- and *para*-positions of the phenyl rings. As a result, the LUMO levels of LD12 and LD14 are above those of LD11 and LD13, respectively. Such information further implies that the *ortho*-substituted porphyrins might have larger V_{OC} and more rapid electron injection than their *meta*-substituted counterparts, to enhance the photovoltaic performance of the corresponding devices, as discussed below.

The LD11–LD14 porphyrins were fabricated into DSSC devices according to procedures reported elsewhere.[4] Fig. 2a and b show current–voltage characteristics and IPCE action spectra of the corresponding devices, respectively; the resulting photovoltaic parameters are summarized in Table 1. Both V_{OC} and J_{SC} of LD12 are significantly greater than those of LD11, leading to 55% enhancement of the overall power conversion efficiency for the two devices (7.43 *vs.* 4.78%). The amounts of dye loading were determined to be 96 and 153 nmol cm^{-2} for LD12 and LD11, respectively, which show a trend opposite to their J_{SC} values (13.235 *vs.* 9.735 mA cm^{-2}). As expected, J_{SC} becomes significantly improved on incorporating the π-conjugated phenylethynyl dimethylamino group for both LD14 and LD13 (19.167 and 18.438 mA cm^{-2}), and V_{OC} of the former is also greater than that of the latter (0.736 *vs.* 0.697 V). Both the enhanced V_{OC} and J_{SC} of the LD14 device yield a remarkable power conversion efficiency, $\eta = 10.17\%$.

The electron-transport kinetics[10] were measured with seven white-light intensities as bias irradiation (powers in a range 10–70 mW cm^{-2}). The intensities of the probe pulse at 655 nm were appropriately attenuated so that the perturbation characteristic of the probe was maintained. For each measurement the probe pulse was focused on the device with the bias irradiation; a quick shutter in the probe path was triggered to block the probe beam so as to determine the zero of reaction duration. The resulting transients are shown in Fig. S3–S10 (ESI†); the corresponding kinetic parameters, determined from fitting the transients according to a procedure introduced previously,[10] are summarized in Tables S2–S5.† Fig. 3a and b show plots of chemical capacitance (C_μ) *vs.* V_{OC} for the LD11/LD12 and the LD13/LD14 systems, respectively; a characteristic exponential rise feature of C_μ as a function of V_{OC} was obtained for each plot. As C_μ is proportional to the density of states of TiO_2 at each V_{OC},[11] the plots shown in Fig. 3 provide direct information about the shift of the conduction band edge of TiO_2 (E_{CB}) upon dye uptake.

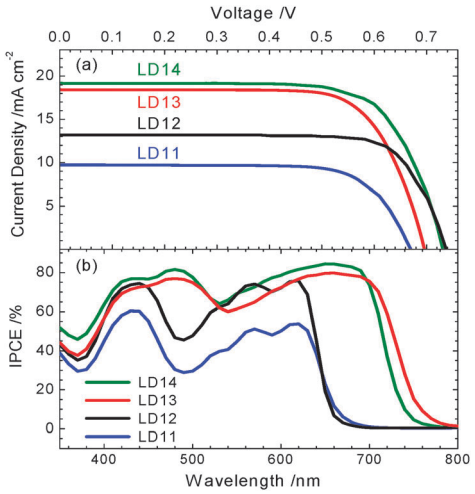

Fig. 2 (a) Current–voltage curves and (b) IPCE action spectra of devices made of LD11–LD14 porphyrins.

Table 1 Photovoltaic parameters of TiO_2 films sensitized with porphyrins LD11–LD14 under simulated AM-1.5G illumination (100 mW cm^{-2}) and an active area of 0.16 cm^2

Dye	J_{SC}/mA cm^{-2}	V_{OC}/mV	FF	η (%)
LD11	9.735	674	0.728	4.78
LD12	13.235	741	0.758	7.43
LD13	18.438	697	0.727	9.34
LD14	19.167	736	0.721	10.17

The results indicate that there exists an apparent potential shift of E_{CB} for each system: E_{CB} of LD12 and LD14 were increased by 34 and 24 meV compared to that of LD11 and LD13, respectively, explaining the enhancement of V_{OC} of the corresponding devices shown in Fig. 2. The observed increased E_{CB} of the *ortho*-substituted devices is consistent with the raised E_{LUMO} of the corresponding porphyrins shown in Fig. 1.

To compare the charge recombination kinetics at the electrolyte/TiO_2 interface for the LD11/LD12 system and the LD13/LD14 system, respectively, Fig. 4a and b show semi-logarithmic plots of electron lifetime (τ_R) *vs.* V_{OC}. Because of the shifts of E_{CB} for the LD12 and LD14 devices, a fair comparison of the degree of charge recombination should be made at the same reference potential level. As a result, the potential scales of τ_R were decreased by 34 and 24 mV for LD12 and LD14, respectively, so that the electron lifetimes could be compared at the same 'equivalent common conduction band' level.[12] The shifted τ_R *vs.* V_{OC} plots of the LD12 and the LD14 devices are indicated as dashed lines in Fig. 4a and b, respectively. After corrections for the shifts of the conduction band edge of TiO_2 for both systems, we still observed τ_R for the *ortho*-substituted porphyrins to be greater than those for their reference compounds; the discrepancy of τ_R between LD13 and LD14 is particularly notable. These results indicate that the *ortho*-substituted long alkoxyl chains play a key role in preventing the approach of I_3^- in the electrolyte to the surface of TiO_2 so as to retard the electron interception in the electrolyte/TiO_2 interface. In addition to the increased E_{CB}, the slower charge recombination is another

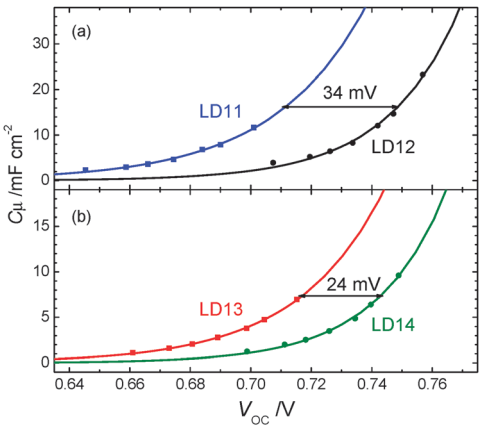

Fig. 3 Plots of chemical capacitance (C_μ) *vs.* open-circuit voltage (V_{OC}) showing the exponential distribution of the density of states of the TiO_2 potential for comparisons of (a) LD11 with LD12 and (b) LD13 with LD14.

factor accounting for the enhanced V_{OC}, as we observed for the LD12 and LD14 devices.

A strategy to improve V_{OC} for organic dyes has always been an issue attracting many profound investigations. For example, Tian and co-workers,[13] who studied cone-shaped organic dyes, observed an enhanced V_{OC} for the dye with a methoxyl group; they speculated that the increased E_{LUMO} might produce deep electron injection for retarded charge recombination. Mori and co-workers[14] found only a little influence on the shift of E_{CB} for devices made of organic dyes and concluded that the smaller V_{OC} of organic sensitizers relative to those of Ru complexes is due mainly to their smaller electron lifetimes. Hagfeldt and co-workers[15] investigated triphenylamino organic dye-based solar cells and made a similar conclusion: varied V_{OC} reflect varied electron lifetimes rather than varied positions of E_{CB}. For zinc porphyrin sensitizers, we observed significant decreases of E_{CB} for porphyrins with a long phenylethynyl link.[9] In the present work, not only the contribution of charge recombination but also the increased E_{CB} through dye uptake should be considered for the observed V_{OC} enhancement.

Porphyrins bearing bulky *ortho*-substituted alkoxylphenyl groups at *meso*-positions of the ring are reported for other

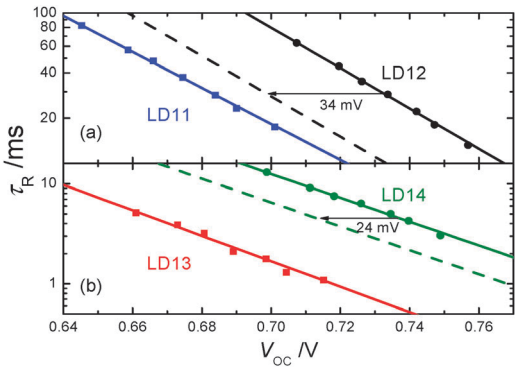

Fig. 4 Plots of electron lifetime (τ_R) *vs.* open-circuit voltage (V_{OC}) showing the degree of charge recombination for comparisons of (a) LD11 with LD12 and (b) LD13 with LD14. The dashed lines show the data of LD12 (a) and LD14 (b) devices with a potential displacement according to the shifts indicated in Fig. 3.

applications[9a,16] because of their great steric hindrance preventing molecular aggregation. For porphyrin-sensitized solar cells, Hupp and co-workers[17] reported that *ortho*-substituted porphyrins with two anchoring groups showed a device performance slightly less than that of an N719 dye. In the present work, such a molecular design was applied for a push–pull porphyrin (LD14) to attain an exceptional cell performance, $\eta = 10.2\%$. According to the crystal structure of an *ortho*-substituted porphyrin reported by Nikiforov *et al.*,[18] we expect that the four dodecoxyl chains in the devices play a key role in wrapping the porphyrin core in a shape that prevents dye aggregation effectively and forms a blocking layer on the TiO_2 surface. The net effect is to increase E_{LUMO} of the molecule, to up-shift E_{CB} of TiO_2 upon dye uptake, and to retard charge recombination in the electrolyte/TiO_2 interface for an enhanced device performance. Work is in progress to incorporate this concept of molecular design for other porphyrins to attain even better device performance.

National Science Council of Taiwan and Ministry of Education of Taiwan, under the ATU program, provided support for this project.

Notes and references

1 (*a*) H. Imahori, T. Umeyama and S. Ito, *Acc. Chem. Res.*, 2009, **42**, 1809; (*b*) M. V. Martínez-Díaz, G. de la Torre and T. Torres, *Chem. Commun.*, 2010, **46**, 7090.
2 T. Bessho, S. M. Zakeeruddin, C.-Y. Yeh, E. W.-G. Diau and M. Grätzel, *Angew. Chem., Int. Ed.*, 2010, **49**, 6646.
3 (*a*) H.-P. Lu, C.-Y. Tsai, W.-N. Yen, C.-P. Hsieh, C.-W. Lee, C.-Y. Yeh and E. W.-G. Diau, *J. Phys. Chem. C*, 2009, **113**, 20990; (*b*) H.-P. Lu, C.-L. Mai, C.-Y. Tsai, S.-J. Hsu, C.-P. Hsieh, C.-L. Chiu, C.-Y. Yeh and E. W.-G. Diau, *Phys. Chem. Chem. Phys.*, 2009, **11**, 10270.
4 C.-L. Wang, Y.-C. Chang, C.-M. Lan, C.-F. Lo, E. W.-G. Diau and C.-Y. Lin, *Energy Environ. Sci.*, 2011, **4**, 1788.
5 A. J. Mozer, P. Wagner, D. L. Officer, G. G. Wallace, W. M. Campbell, M. Miyashita, K. Sunahara and S. Mori, *Chem. Commun.*, 2008, 4741.
6 Z. Ning, Y. Fu and H. Tian, *Energy Environ. Sci.*, 2010, **3**, 1170.
7 (*a*) C.-F. Lo, L. Luo, E. W.-G. Diau, I.-J. Chang and C.-Y. Lin, *Chem. Commun.*, 2006, 1430; (*b*) C.-Y. Lin, C.-F. Lo, L. Luo, H.-P. Lu, C.-S. Hung and E. W.-G. Diau, *J. Phys. Chem. C*, 2009, **113**, 755.
8 C.-F. Lo, S.-J. Hsu, C.-L. Wang, Y.-H. Cheng, H.-P. Lu, E. W.-G. Diau and C.-Y. Lin, *J. Phys. Chem. C*, 2010, **114**, 12018.
9 (*a*) K. E. Splan and J. T. Hupp, *Langmuir*, 2004, **20**, 10560; (*b*) X. Huang, C. Zhu, S. Zhang, W. Li, Y. Guo, X. Zhan, Y. Liu and Z. Bo, *Macromolecules*, 2008, **41**, 6895.
10 L. Luo, C.-J. Lin, C.-S. Hung, C.-F. Lo, C.-Y. Lin and E. W.-G. Diau, *Phys. Chem. Chem. Phys.*, 2010, **12**, 12973.
11 B. C. O'Regan, S. Scully, A. C. Mayer, E. Palomares and J. Durrant, *J. Phys. Chem. B*, 2005, **109**, 4616.
12 F. Fabregat-Santiago, G. Garcia-Belmonte, I. Mora-Seró and J. Bisquert, *Phys. Chem. Chem. Phys.*, 2011, **13**, 9083.
13 Z. Ning, Q. Zhang, H. Pei, J. Luan, C. Lu, Y. Cui and H. Tian, *J. Phys. Chem. C*, 2009, **113**, 10307.
14 M. Miyashita, K. Sunahara, T. Nishikawa, Y. Uemura, N. Koumura, K. Hara, A. Mori, T. Abe, E. Suzuki and S. Mori, *J. Am. Chem. Soc.*, 2008, **130**, 17874.
15 T. Marinado, K. Nonomura, J. Nissfolk, M. K. Karlsson, D. P. Hagberg, L. Sun, S. Mori and A. Hagfeldt, *Langmuir*, 2010, **26**, 2592.
16 (*a*) J. L. O'Donnell, N. Thaitrong, A. P. Nelson and J. T. Hupp, *Langmuir*, 2006, **22**, 1804; (*b*) C. Arunkumar, P. Bhyrappa and B. Varghese, *Tetrahedron Lett.*, 2006, **47**, 8033.
17 C. Y. Lee, C. She, N. C. Jeong and J. T. Hupp, *Chem. Commun.*, 2010, **46**, 6090.
18 M. P. Nikiforov, U. Zerweck, P. Milde, C. Loppacher, T.-H. Park, H. T. Uyeda, M. J. Therien, L. Eng and D. Bonnell, *Nano Lett.*, 2008, **8**, 110.

